AFWAL-TR-82-3086

A GRAPHIC METHOD FOR PREDICTING AUDIBILITY OF NOISE SOURCES

BOLT BERANEK AND NEWMAN INC.
21120 VANOWEN STREET
CANOGA PARK, CALIFORNIA 91303

OCTOBER 1982

FINAL REPORT FOR PERIOD JUNE 1982 - OCTOBER 1982

FLIGHT DYNAMICS LABORATORY
AIR FORCE WRIGHT AERONAUTICAL LABORATORIES
AIR FORCE SYSTEMS COMMAND
WRIGHT-PATTERSON AIR FORCE BASE, OHIO 45433

NOTICE

This technical report has been reviewed and is approved for publication.

Leonard L Shaw

LEONARD L. SHAW, Aero Engr
Acoustics & Sonic Fatigue Group
Structural Integrity Branch
Structures & Dynamics Division

Davey L Smith

DAVEY L. SMITH, Chief
Structural Integrity Branch
Structures & Dynamics Division

FOR THE COMMANDER

Ralph L Kuster

RALPH L. KUSTER, JR., Col, USAF
Chief, Structures & Dynamics Division

Unclassified

SECURITY CLASSIFICATION OF THIS PAGE (When Data Entered)

REPORT DOCUMENTATION PAGE		READ INSTRUCTIONS BEFORE COMPLETING FORM
1. REPORT NUMBER AFWAL-TR-82-3086	2. GOVT ACCESSION NO. AD-A123736	3. RECIPIENT'S CATALOG NUMBER
4. TITLE (and Subtitle) GRAPHIC METHOD FOR PREDICTING AUDIBILITY OF NOISE SOURCES		5. TYPE OF REPORT & PERIOD COVERED Final / June-October 1982
		6. PERFORMING ORG. REPORT NUMBER BBN 4954
7. AUTHOR(s) Sanford Fidell, Richard Horonjeff		8. CONTRACT OR GRANT NUMBER(s) F33615-82-M-3221
9. PERFORMING ORGANIZATION NAME AND ADDRESS Bolt Beranek & Newman Inc. 10 Moulton Street Cambridge, Massachusetts 02238		10. PROGRAM ELEMENT, PROJECT, TASK AREA & WORK UNIT NUMBERS 24010165
11. CONTROLLING OFFICE NAME AND ADDRESS Flight Dynamics Laboratory (AFWAL/FIBE) Air Force Wright Aeronautical Laboratories (AFSC) Wright-Patterson AFB OH 45433		12. REPORT DATE October 1982
		13. NUMBER OF PAGES 37
14. MONITORING AGENCY NAME & ADDRESS(if different from Controlling Office)		15. SECURITY CLASS. (of this report) Unclassified
		15a. DECLASSIFICATION/DOWNGRADING SCHEDULE

16. DISTRIBUTION STATEMENT (of this Report)

Approved for public release; distribution unlimited.

17. DISTRIBUTION STATEMENT (of the abstract entered in Block 20, if different from Report)

18. SUPPLEMENTARY NOTES

19. KEY WORDS (Continue on reverse side if necessary and identify by block number)

Acoustics, Audibility, Detection, Prediction

20. ABSTRACT (Continue on reverse side if necessary and identify by block number)

This report provides the technical rationale for revision of a chart developed by Fidell, Pearsons, and Bennett (1972). This chart expresses the relationships between signal-to-noise ratio and frequency that govern detectability of acoustic signals by human observers. The chart permits a user: 1) to predict the frequency region of a spectrum that is most detectable in any given ambient noise background; 2) to quantify the degree of detectability of the signal in question; and 3) to estimate reduction in signal-to-noise ratio necessary to render the signal undetectable.

DD FORM 1 JAN 73 1473 EDITION OF 1 NOV 65 IS OBSOLETE

Unclassified

SECURITY CLASSIFICATION OF THIS PAGE (When Data Entered)

TABLE OF CONTENTS

Page

I. Introduction....................................1

A. Purpose of Report...............................1
B. Organization of Report..........................1

II. Technical Discussion...........................2

A. Historical Perspective..........................2
B. Inadequacy of Threshold Concept.................3
C. Psychophysical Theory of Signal Detectability......4
D. Theoretical Account of Masking Signals by Noise....9

III. Rationale for Revised Graphic Prediction Method......15

A. Relationship between Effective Masking Bandwidth and Frequency..........................16
B. Relationship between η and Signal Frequency.......17
C. Construction of Chart...........................20

IV. Guide to Use of the Chart......................23

A. Instructions for Use............................23
B. Special Cases...................................26
1. Alternate Probabilities of Hits and False Alarms..................................26
2. Multiple Frequency Bands of Equal Detectability..............................27
3. Tones and Narrowband Signals.................27
4. Unusually Short or Long Duration Signals......................................29
C. Example of Use..................................31

I. INTRODUCTION

A. Purpose of Report

This report provides the technical rationale for revision of a chart developed by Fidell, Pearsons, and Bennett (1972). This chart expresses the relationships between signal-to-noise ratio and frequency that govern detectability of acoustic signals by human observers. The chart permits a user 1) to predict the frequency region of a spectrum that is most detectable in any given ambient noise background; 2) to quantify the degree of detectability of the signal in question, and 3) to estimate reduction in signal-to-noise ratio necessary to render the signal undetectable.

Revision of the chart was undertaken to incorporate new scientific findings, and to make its use simpler and more widely applicable.

B. Organization of Report

To present the technical basis for the new chart as clearly as possible, no familiarity with use of the prior chart is assumed. Instead, the necessary theoretical background is provided in Section II. Section III then provides a specific rationale for the construction of the chart. Section IV is a step-by-step guide to use of the revised chart.

II. TECHNICAL DISCUSSION

A. Historical Perspective

Human abilities to detect sounds have been studied more or less formally for over one hundred years. Early views of detection tended to be deterministic: detection was viewed as an all-or-none process. The concept of an "auditory threshold" or a "threshold of hearing" provided the early basis for discussions of detection. In its simplest form, a "threshold of hearing" was taken to be a single level of physical stimulation which invariably gave rise to auditory sensations. Licklider (1951) summarizes many of the better efforts to define the physical values of the threshold as a function of signal frequency.

When electronic instrumentation for acoustic measurement became available after World War I, it was recognized that in many real world detection problems, masking of a target spectrum by ambient noise is more important than absolute sensitivity in determining the audibility of sounds. Wegel and Lane's (1924) account of the masking of pure tones by pure tones received considerable attention from its publication through the World War II years, inspiring further research on masking by noise (e.g., Fletcher, 1940; Hawkins and Stevens, 1950). This line of research led to the "critical band" conception. A critical band defines the frequency limits within which noise energy masks the detectability of a signal of a given frequency. Noise energy outside this band does not render a signal less audible.

A number of deterministic schemes for predicting the audibility of acoustic signals, based on combinations of threshold and

critical band concepts, descend from this line of research. Examples of this sort of prediction scheme include those of Loewy (1963), Smith and Paxson (1970), Ollerhead (1971), and Abrahamson (1975).

B. Inadequacy of Threshold Concept

A fundamental problem with all threshold-related approaches to predicting human detection performance is that they are deterministic, and hence, unable to deal with the probabilistic nature of all real world detectors. It is important to understand this basic limitation, because one cannot otherwise appreciate the compensatory relationship between the various forms of correct and incorrect detection performance.

Consider a simple detection problem in which the observer's task is to decide whether or not a signal is present during a well defined observation interval. The observer's two decisions ("signal absent" and "signal present") can be tabulated against the actual presence or absence of the signal as shown in Table I.

TABLE I: CATEGORIZATION OF DETECTION DECISION OUTCOMES

	Actual State of Affairs	
Observer's Decision	Signal Absent	Signal Present
Signal Absent	Correct Rejection	Miss
Signal Present	False Alarm	Hit

Note that there are *two* types of correct decisions and *two* types of incorrect decisions in this table. When a signal actually is absent, a correct detection decision consists of asserting its absence, but when a signal actually is present, a correct detection decision consists of asserting its presence. There are obviously two forms of incorrect detection decisions as well. The names given to the decision outcomes in Table I are terms in widespread use. In statistical parlance, a "Miss" is usually called a Type I error, while a "False Alarm" is called a Type II error.

Figure 1 plots the probability of hits (on the ordinate) against the probability of false alarms (on the abscissa) in a format, known as a Receiver Operating Characteristic. This presentation exhausts all the information contained in Table I about an observer's long term detection performance. Several inferences may be drawn from Figure 1. First, the figure makes clear that arbitrarily high hit rates can be achieved by any detector, although only at the cost of similarly high false alarm rates. Second, the figure shows that an observer of fixed sensitivity can display a wide variety of detection performances, ranging from very conservative (low probabilities of hits and false alarms) to very radical (high probabilities of hits and false alarms). Third, it is the *ratio* of hits to false alarms that is the proper metric of the true sensitivity of an observer.

C. Psychophysical Theory of Signal Detectability

The best developed theoretical account of the detection performance of human observers was initially described by Swets, Tanner, and Birdsall (1955), and formalized by Green and Swets (1966). This theoretical model clearly

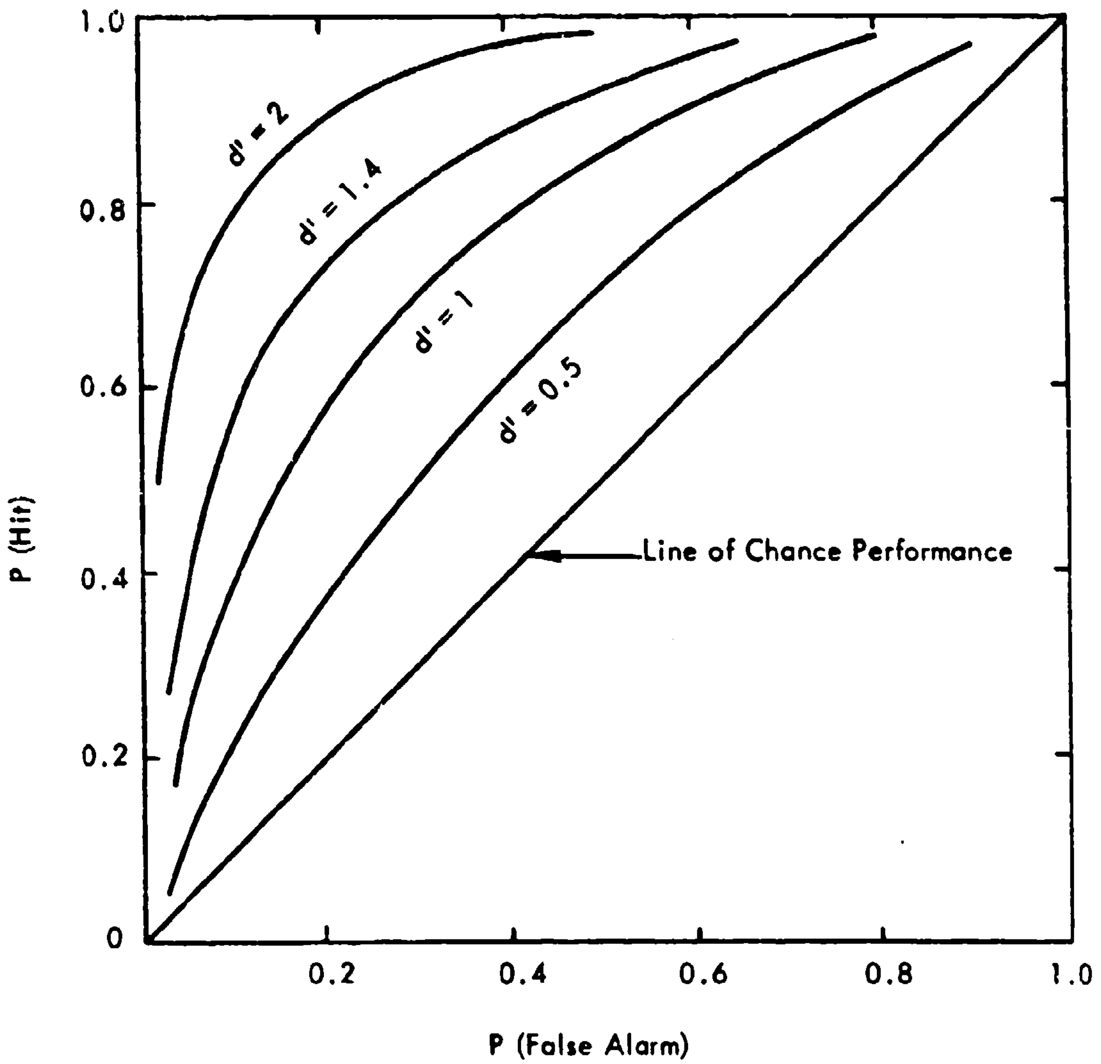

FIGURE 1. A FAMILY OF RECEIVER OPERATING CHARACTERISTIC CURVES

differentiates response bias (the willingness to report the presence or absence of a signal independently of any physical information about the signal) from true sensitivity to physical information about the occurrence of a signal. This is accomplished in statistical decision-theoretical terms, as shown schematically in Figure 2.

Figure 2 is a schematic representation of the underlying distributions of information that account for the variability in detection performance seen in Figure 1. In this model, an observer attempting to detect a signal in noise must decide whether an observation consists of noise alone, or signal plus noise. This can be accomplished by establishing a likelihood ratio criterion; i.e., a ratio of probabilities that an observation belongs to each distribution. Observations that produce likelihood ratios greater than a chosen criterion are judged to contain a signal; those that produce likelihood ratios smaller than a criterion are judged to contain noise alone. The criterion value adopted for any detection decision is influenced solely by the costs and payoffs of the four decision outcomes of Table I, and not by the observation itself.

The likelihood ratio criterion in Figure 2 is shown at a value of 1; that is, at the point where it is equally likely that an observation arises from the distribution of noise alone or from the distribution of signal plus noise. This value of the decision criterion produces decisions based on physical information alone. Values of the decision criterion to the right of the position shown in Figure 2 produce a bias toward reporting the absence of a signal, while values of the decision criterion to the left of this position produce a bias toward reporting the presence of a signal. Such biases can be entirely rational, given the cir-

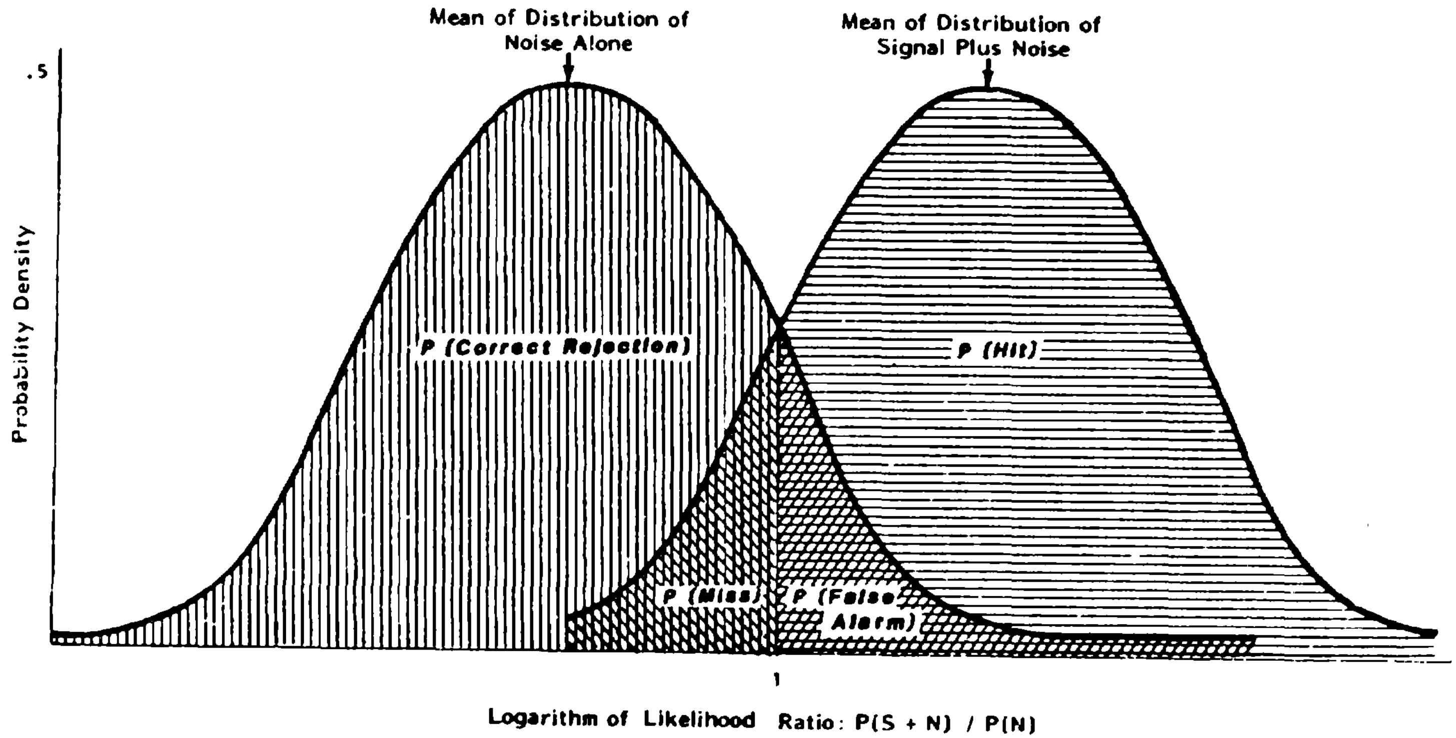

FIGURE 2. UNDERLYING DISTRIBUTIONS OF INFORMATION ABOUT SIGNAL OCCURRENCE

cumstances of the detection task.

The position of the likelihood ratio criterion has nothing at all to do with the observer's sensitivity, however. Sensitivity is determined by the distance between the means of the two distributions in Figure 2. When normalized by the standard deviation of the noise distribution, this distribution may be expressed as a scalar quantity, referred to in the signal detection literature as d'.

Specific probabilities of hits and false alarms can be associated with each value of d'. For example, in the detection task under consideration here, a d' value of 2.32 corresponds to a probability of correct detection (a hit) of 0.50 and an associated probability of a false alarm of 0.01. A report of the presence of a signal from an observer as sensitive as this would be 50 times more likely to represent a hit than a false alarm. However, the same observer would fail to report fully half of the bona fide signal occurrences.

If ten times as many false alarms could be tolerated (p(false alarm)=0.10, rather than 0.01), this same observer could correctly report 85% of the bona fide signal occurrences, rather than only half of them. In short, an observer of fixed sensitivity (d'=k) can operate at any point along its ROC curve. An observer of fixed sensitivity *cannot*, however, achieve a higher ratio of hits to false alarms (values toward the upper left hand corner of Figure 1) than those bounded by his ROC curve.

D. Theoretical Account of Masking of Signals by Noise

Within the framework of the Theory of Signal Detectability, masking is usually accounted for by assuming that human observers detecting acoustic signals embedded in wide band noise employ a hypothetical first stage bandpass filter. This filter's limited bandwidth improves the effective signal-to-noise ratio of the detection process by allowing observers to restrict their attention to a narrow band of frequencies in the vicinity of the signal. Thus, noise energy in other spectral regions does not degrade detection performance.

At higher frequencies (above 1000 Hz), the apparent bandwidth of the hypothetical first stage auditory filter seems to increase as a constant percentage of frequencies (constant Q system). However, at frequencies below several hundred Hz, there is greater uncertainty about the relationship between the filter's bandwidth and signal frequency. Measurements of the masking of sinusoids by noise at frequencies below 400 Hz are sparse, as seen in Figure 3. These data are also subject to alternative explanation, as discussed by Fidell, Horonjeff, Teffeteller, and Green (1982).

In addition to this empirical uncertainty, there is also some diversity of theoretical opinion about how to model human frequency selectivity in detection tasks. Most researchers, however, attribute to Fletcher the view that detection occurs when signal power is directly proportional to the power passing through the hypothetical first stage auditory filter, as described in Equation 1:

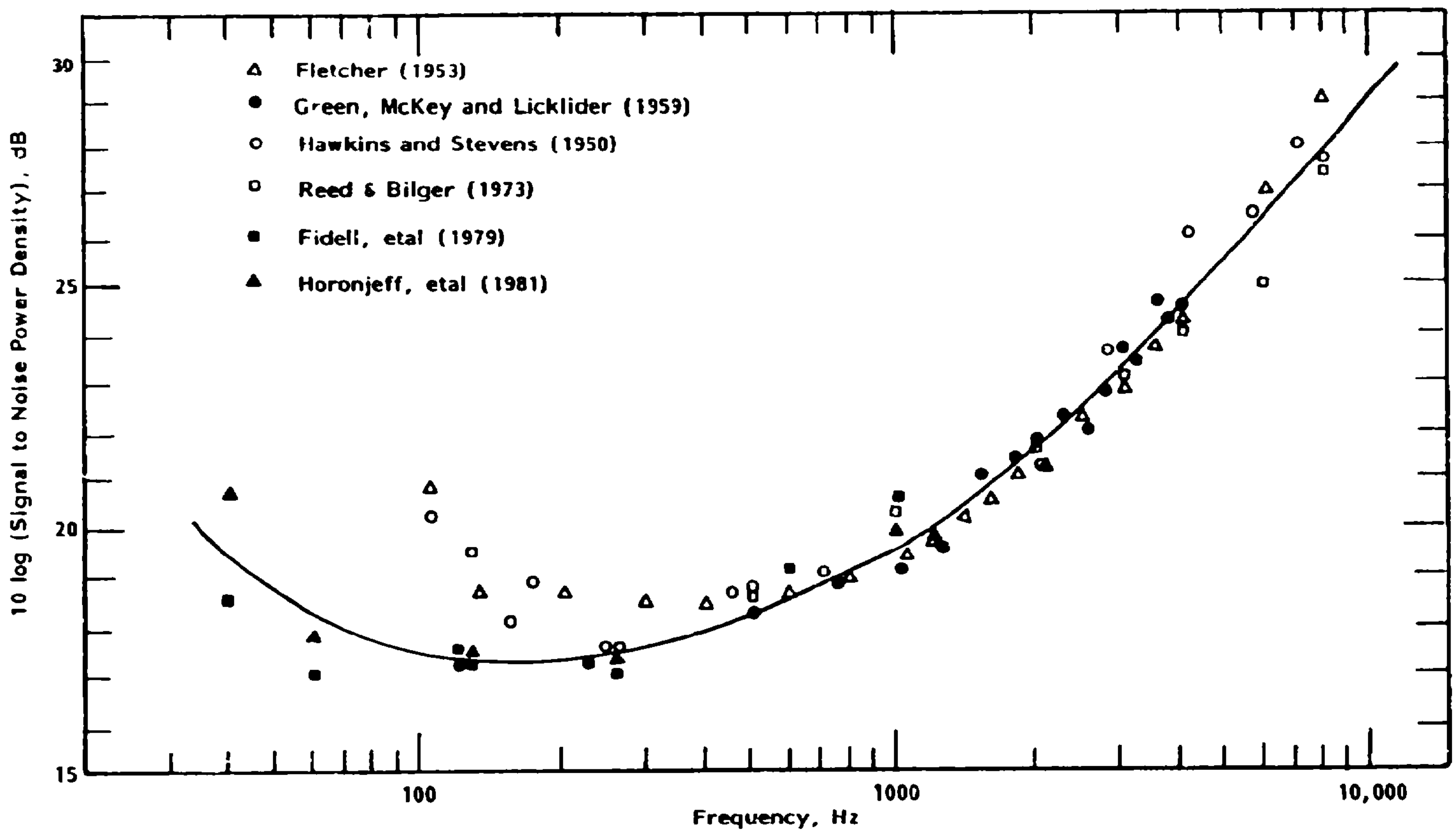

FIGURE 3. CRITICAL RATIO ESTIMATES OF EFFECTIVE MASKING BANDWIDTHS AS A FUNCTION OF FREQUENCY NORMALIZED TO N_o = 40dB

$$P_s = K \int_0^\infty |N(f)/H(f)|^2 \, df, \qquad \text{(Eq. 1)}$$

where P_s is the signal power at detection, N(f) is the noise power entering the ear, H(f) is a weighting function representing the attenuation characteristic of the auditory filter, and K is the reciprocal of the observer's efficiency as a power detector.

A modern model based on this view suggests in effect that people listen for the signal through a bank of closely spaced, narrow band filters; make independent likelihood assessments of the presence or absence of the signal at the output of each filter; and orthogonally vector sum the likelihoods to obtain a composite likelihood estimate across the frequency spectrum.

Mathematically this process is conveniently described by equations 2 and 3. With noise alone applied to the input, the output of any given filter exhibits a time varying mean square level (given a finite average time, say a few hundred milliseconds) with a long term value μ and a variance σ^2. If a small amount of signal is added to the input the long term mean square value at the output will also increase, with negligible impact on σ. Detection, however, depends not on the absolute change in mean square level, $\Delta\mu$, but its relation to the variance, $\Delta\mu/\sigma$ (Green and Swets, 1966). An analogy in which band limited Gaussian noise is applied to a meter illustrates the point. If the meter reading is fluctuating only 0.5 dB it is far easier to detect a 1 decibel change to its input than if the meter is fluctuating 5 dB.

At the filter output, $\Delta\mu$ depends on the signal-to-noise ratio, and σ on the filter bandwidth (the wider the bandwidth, the smaller

the σ). The ratio of $\Delta\mu/\sigma$ is thus an index of detectability, d', that may be conveniently calculated for a frequency band of finite width by

$$d' = \eta \, W^{1/2} \, S/N \qquad \text{(Eq. 2)}$$

where S/N is the average root mean square signal-to-noise ratio at the filter output, W is the effective (or equivalent rectangular) bandwidth of the filter, and η is an efficiency factor (taken to be approximately 0.4 for present purposes but shown to be somewhat frequency dependent by Fidell, Horonjeff, Teffeteller, and Green (1982)).

Note that Equation 2 behaves in a manner consistent with the foregoing discussion. Holding background noise and bandwidth constant, d' is directly proportional to signal level (at least for signal levels for which the variance of the signal plus noise condition is not significantly different from the case with noise alone). If, on the other hand, signal-to-noise ratio is held constant, d' also increases with increasing bandwidth (reflecting the decrease in variance associated with the increased number of degrees of freedom).

Although Equation 2 provides a model for predicting detection performance within a single auditory masking band, it does not address the issue of how detection information in multiple bands is combined. Garner (1947) postulated (and Green et al., 1959 later confirmed) that people are better energy detectors if the signal to be detected is concentrated in a narrow spectral region. Within an auditory filter band, power summation appears to be perfect, but across bands a less efficient statistical

process is probably employed. Equation 3 reflects the empirical findings of Green et al. (1959) by treating the d' values of each filter as independent observations. The composite detectability, d'_c, is computed as the square root of the sum of the squares

$$d'_c = \left[\sum_{i=1}^{n} (d'_i)^2 \right]^{\frac{1}{2}} \qquad \text{(Eq. 3)}$$

where d' is the detectability index in the ith frequency band and N is the number of frequency bands. This model accounts for the findings of Schafer and Gales (1949) and Green (1958).

To a first approximation, the auditory filter bank may be considered as a set of non-overlaping (i.e., uncorrelated) filters separated in center frequency by the average bandwidth of two adjacent filters. Recent evidence suggests that the filter set may be conveniently modeled as constant percentage bandwidth, on the order of 1/6 to 1/10th octave in width. Over a limited frequency range this narrow width implies that adjacent filters are of nearly constant bandwidth.

Equations 2 and 3 provide a good approximation to human abilities to detect broadband signals in broadband noise. Listening for broadband signals in noise is one of the most common acoustic detection problems encountered in everyday life. Many transportation noise sources produce acoustic energy in relatively wide spectral regions. For example, reciprocating and rotational engine noise, propeller noise, jet exhaust noise, and track or tire noise are all characterized by radiation of appreciable

acoustic energy over frequency ranges an octave or more in bandwidth. Some sources may concentrate radiated energy within narrower bands, but harmonics and multiple sources on most real-world noise sources radiate energy over a wider band of frequencies as well.

A number of simplifying assumptions and corrections are necessary to produce a convenient graphic representation of the terms of Eq. 2. These include the following:

1) physical information about the spectral distributions of signal and noise energy is not available to a resolution greater than one-third octave;

2) the energy mean sound pressure levels of time varying distributions of signal and noise level suffice to characterize S and N; and

3) in everyday signal detection tasks, a human observer is approximately 40% as efficient as an ideal energy detector.

Under these conditions, the detection performance of human observers can be modeled as seen in Figure 6.

III. RATIONALE FOR REVISED GRAPHIC PREDICTION METHOD

To produce a simple chart that permits a user to predict acoustic detectability, empirical data must be interpreted to make a number of estimates based on the theory discussed in the preceding section. These approximations require decisions about 1) the relationship between effective masking bandwidth and signal frequency, and 2) the efficiency of an observer as a function of signal frequency. The decisions are necessary because the information on effective masking bandwidths seen in Figure 3 is determined not only by a simple relationship with signal frequency, but also by the observer's efficiency.

Recall from Equation 2 that detectability is the product of three terms: η (the observer's efficiency relative to an ideal energy detector), masking bandwidth, and the signal-to-noise ratio at the output of the hypothetical auditory filter:

$$d' = \eta \; W \quad S/N^{\frac{1}{2}} \qquad \text{(Eq. 2)}$$

The latter quantity, S/N, is not the quantity plotted on the ordinate of Figure 3. Instead, Figure 3 plots the ratio of signal level to noise power density (i.e., noise power per unit bandwidth, in dB per Hz), or S/N_o. Equation 4 shows that the total noise level at the internal filter's output (N) is the product of the noise power density and the filter's bandwidth:

$$N = N_o \; W \qquad \text{(Eq. 4)}$$

It is assumed for present purposes that the noise power density is uniform within effective masking bandwidths.

Substituting Equation 4 into Equation 2 and rearranging terms yields Equation 5:

$$S/N_o = d' \; W^{\frac{1}{2}}/\eta \qquad \text{(Eq. 5)}$$

Interpreting the curve drawn in Figure 3 in terms of Equation 5, it can be seen that for constant detection performance ($d'=k$) at all frequencies, the signal to noise power density ratio (S/N_o) is proportional to the square root of the effective masking bandwidth ($W^{\frac{1}{2}}$), and inversely proportional to the observer's efficiency (η). Both of these terms (W and η) can be considered frequency dependent. The next subsection treats the frequency dependence of W.

A. Relationship between Effective Masking Bandwidth and Frequency

Data from specialized detection studies (e.g., Weber (1977), Patterson (1976), and Horonjeff et al (1980)) must be analyzed to assess the frequency dependence of W and η independently. In such studies, observers attempt to detect sinusoidal signals embedded in Gaussian noise distributions that lack masking energy in the immediate frequency region of the signal. These so-called "notched noise" experiments permit an inference of the *shape* of the internal auditory filter, and thus its equivalent rectangular bandwidth at different signal frequencies. Such inferences cannot be drawn from studies of detection performance in spectrally continuous noise.

The major findings of notched noise studies confirm that effective masking bandwidth is a strong function of frequency. However, the notched noise studies also indicate that effective masking bandwidth is also a function of absolute signal level. Figure 4 summarizes BBN's interpretation of these data. The figure infers equivalent rectangular masking bandwidths as functions of both signal frequency and absolute noise power density (N_0). To provide a frame of reference, the plot also shows bandwidths of full and one-third octaves on the same axes.

Note that as the masking noise level increases, so does the effective masking bandwidth. These relationships provide a means for estimating bandwidth in Equation 2 as functions of frequency and level.

B. Relationship between η and Signal Frequency

For the sake of simplicity (and in the absence of any empirical evidence to the contrary), it is assumed that the observer's efficiency is independent of signal level. Given bandwidth information, it is therefore possible to infer the value of η from Equation 2, by division:

$$\eta = d' \, W^{\frac{1}{2}} \, S/N_c \qquad \text{(Eq. 6)}$$

This is equivalent to dividing the square root of the values plotted in Figure 4 (for N_0 = 40 dB) by the values of the curve shown in Figure 3 (also for N_0 = 40 dB). The resulting relationship may be seen in Figure 5.

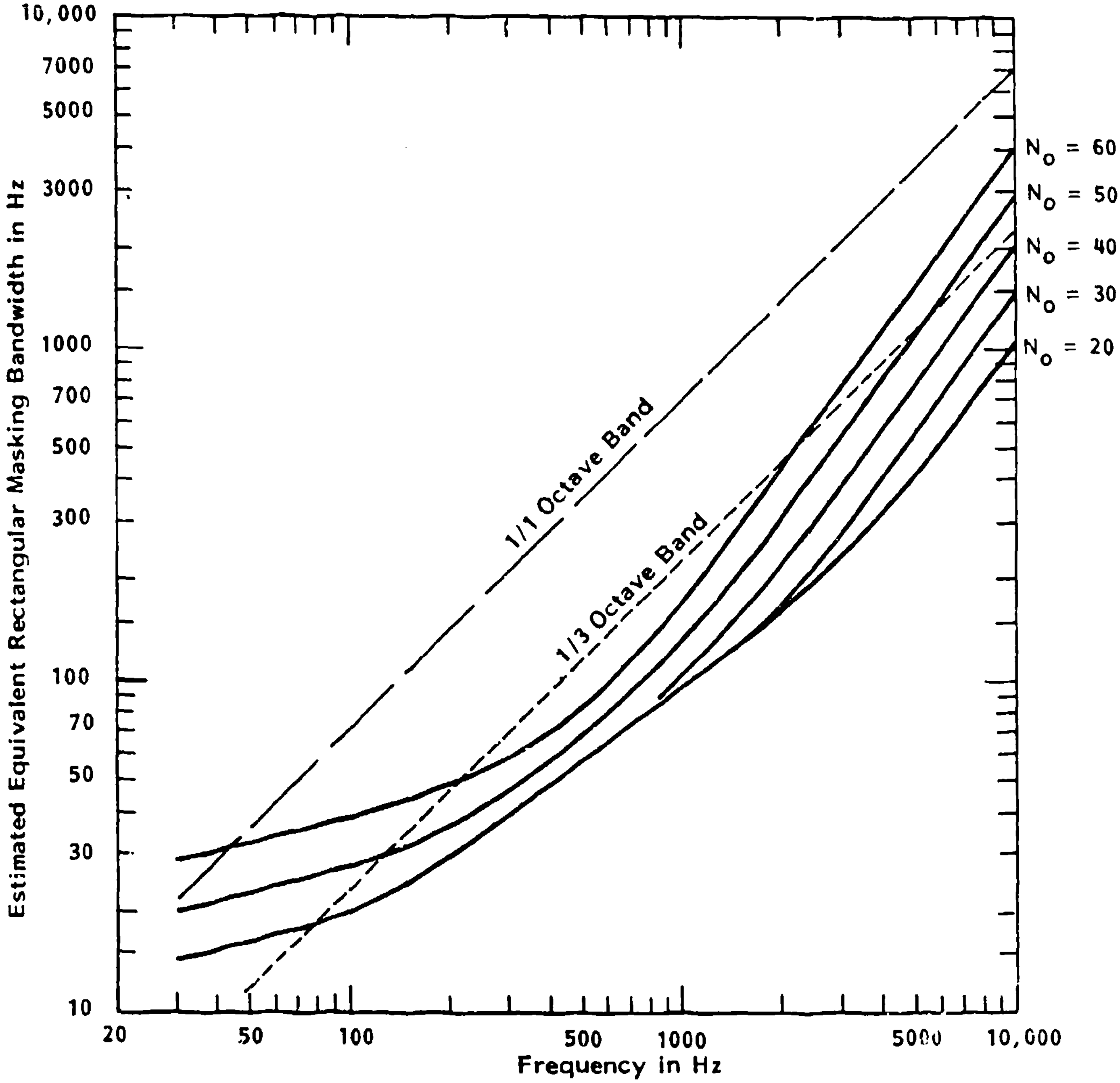

FIGURE 4. ESTIMATED EQUIVALENT RECTANGULAR AUDITORY MASKING BANDWIDTH AS A FUNCTION OF FREQUENCY AND MASKER SPECTRUM LEVEL IN HERTZ

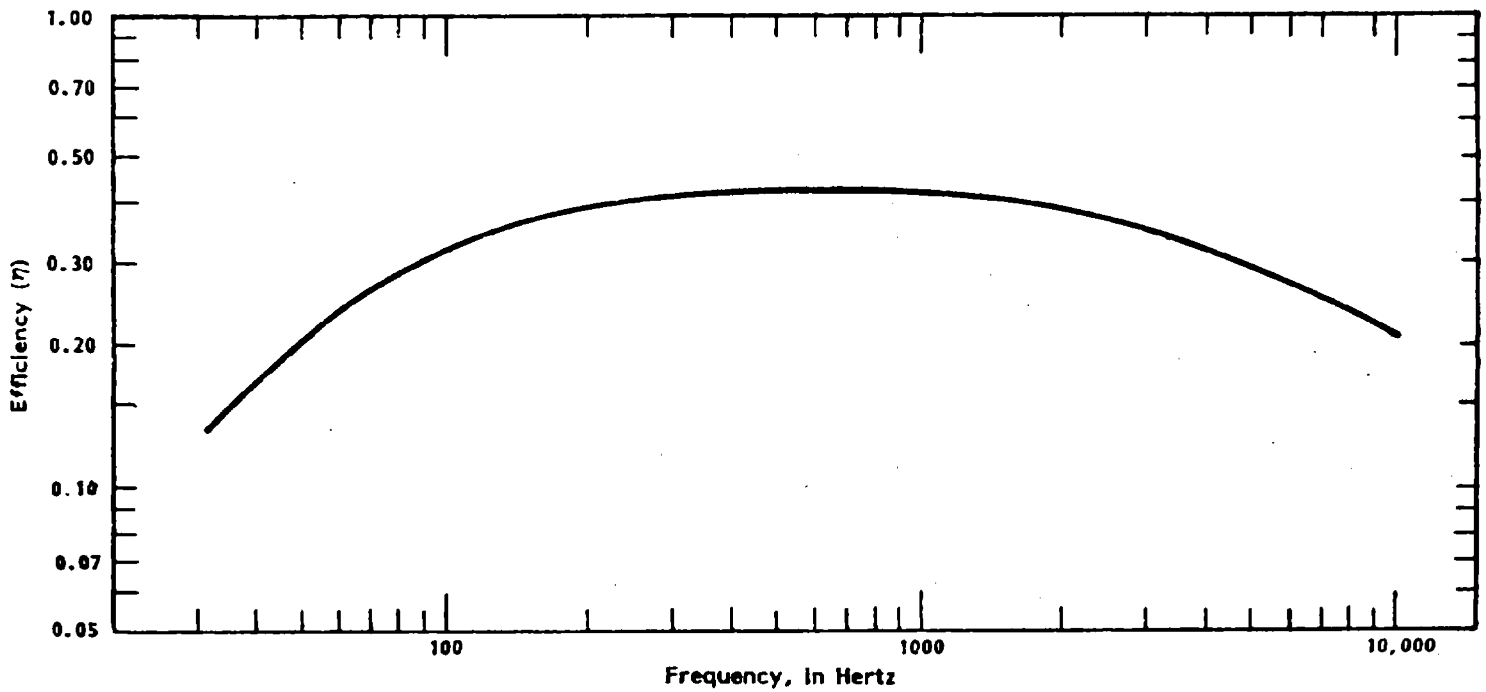

FIGURE 5. ESTIMATED OBSERVER DETECTION EFFICIENCY AS A FUNCTION OF FREQUENCY

C. Construction of Chart

To predict signal spectrum levels required for constant detection performance, a graph must be prepared that plots such levels as functions of frequency and absolute sound pressure level. On such a graph, a signal that exceeds the level of masking noise at any point in its spectrum will be at least as detectable as the criterion level of detection performance. For general purposes, the criterion of detectability is taken to be a probability of correct detection of 0.50, and a probability of a false alarm of 0.01. This level of detectability corresponds to the general notion of a "threshold" of audibility.

For reasons of simplicity and practicality, all spectral information is characterized in one-third octave bands in the graphic prediction method. One-third octave bands may be smaller, equal, or greater in bandwidth than the equivalent rectangular bandwidth of the internal auditory filter at different frequencies. Thus, the relationships expressed in Figures 4 and 5, and in Eq. 2, must be compensated in relation to one-third octave bandwidths.

The values of the curves plotted in Figure 6 represent signal levels derived from Equation 7:

$$S = d'/\eta \, W^{\frac{1}{2}} \, N \qquad \text{(Eq. 7)}$$

The value of S plotted in the curves of Figure 6 at any frequency and absolute level clearly depends on the specified level of detection performance ($d' = 2.32$, corresponding to probabilities of correct detection and false alarms of 0.50 and 0.01, re-

spectively); the masking noise level (N), the observer's efficiency (η, as shown in Figure 5), and bandwidth. However, this bandwidth is in turn determined by the relationship between a one-third octave band and the equivalent rectangular bandwidth of the auditory filter (cf. Figure 4) at any frequency.

If the equivalent rectangular bandwidth of the auditory filter was greater than a one-third octave band, the equivalent rectangular bandwidth of the auditory filter was used to calculate the value of the curved line plotted in Figure 6. Otherwise, the one-third octave bandwidth was used to plot the value of the curved lines of Figure 6. At very low frequencies and high absolute levels, the bandwidth was limited to a full octave.

This procedure for determining the values of the curved lines of Figure 6 is valid for the bulk of the anticipated uses of the prediction chart. These general uses are characterization of the detectability of broadband signals embedded in broadband noise. A minor adjustment to the plotted signal level values is necessary in the case of a signal composed of pure tones, as discussed in Section IV.

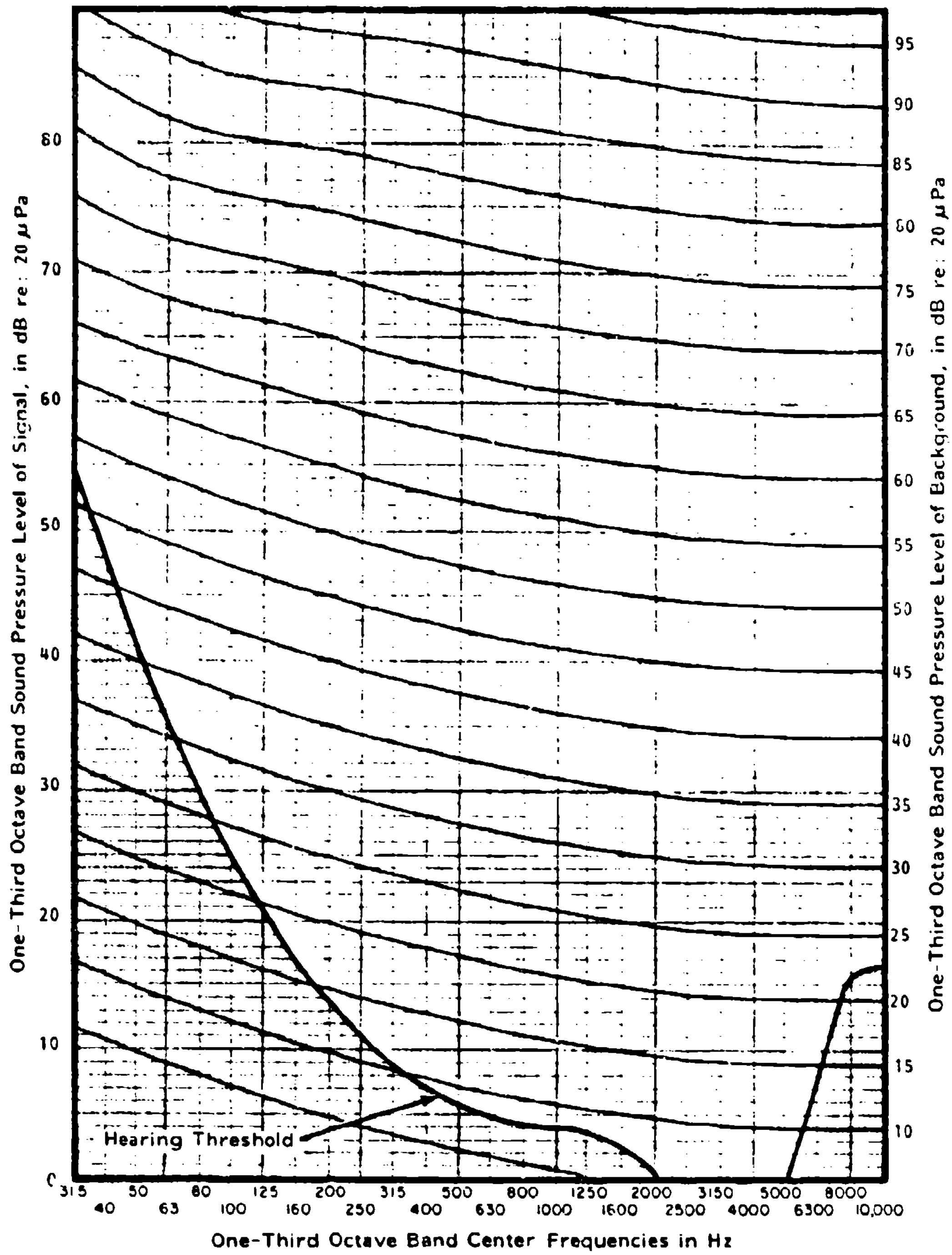

FIGURE 6. CHART FOR PREDICTING HUMAN AUDIBILITY OF SIGNALS IN NOISE
SEE INSTRUCTIONS FOR USE ON REVERSE

IV. GUIDE TO USE OF THE CHART

A. Instructions for Use

Figure 6 is used to predict the detectability of one signal in the presence of a continuous background noise. Whether or not the signal is detectable depends on the relationship between the unweighted frequency composition of the signal and the frequency-weighted composition of the noise in which it occurs. The chart applies to one-third octave band rms sound pressure level measurements within the frequency range of 31 to 10,000 Hz.

The masking noise spectrum is plotted using the curved grid lines and the sound level scale on the right side of the grid. The curved grid lines reflect the necessary frequency weighting. The curved grid lines are drawn only at 5 decibel intervals to maintain readability of the graph. Interpolation between these 5 dB grid lines is performed using the underlying 1 dB signal spectrum grid.

The one-third octave band levels of the masking noise should be long term rms values. Averaging times of 30 to 60 seconds are sufficient in most cases. The longer averaging times should be used if it is anticipated that the signal will be most detectable at low frequencies (e.g., below 100 Hz). The signal spectrum is plotted using the rectangular grid and the sound level scale on the left side of the chart. For continuous steady state signals, long term rms sound levels should be plotted (as for the masking noise spectrum). For continuous, time fluctuating signals, the rms signal levels may underestimate those periods of several seconds when the signal levels are higher than average,

and upon which detection is likely to depend. In such cases, it is advisable to plot a high centile sound level (such as L_{10}, the level exceeded only 10 percent of the time) for each band. If centile sound levels are used, they should be determined from a distribution of rms levels of averaging time of 1 to 2 seconds, corresponding approximately to the "slow" sound level meter response.

Yet a third category of signal is a transient one, such as an aircraft flyover, or automobile passby. This type of event is maximally detectable only when the sound level is near its highest level. In this case, it is important that the averaging time of the measuring instrument be at least 1 to 2 seconds. The highest one-third octave band rms levels in the time history should then be plotted.

Signal detectability is evaluated after both signal and background spectra have been plotted. When the plot of the signal level spectrum is tangent to the plot of the noise level spectrum, a human observer would correctly detect such a signal 50% of the time, with a 1% false alarm rate. When the plotted signal spectrum exceeds the plotted noise spectrum in any one-third octave band, the signal can be correctly detected more than 50% of the time, or with a false alarm rate of less than 1%. Conversely, when the plotted noise spectrum exceeds the plotted signal spectrum in all one-third octave bands, then the signal can be correctly detected less than 50% of the time, or with a false alarm rate greater than 1%.

Absolute sound levels, whether of signal or noise, that are within the darkened area at the bottom of the chart's grid are

considered inaudible on the basis of audiometric standards. Any portion of a signal's spectrum plotted in the darkened area cannot therefore contribute to the audibility of the signal. The only reason that signal levels should be plotted in the darkened area is to determine how much *greater* they would have to be in level to contribute to audibility.

B. Special Cases

The theory upon which Figure 6 is based was developed for the general case of detecting broadband signals in the presence of broadband noise. For certain other types of detection problems, predictions based upon the chart may be in error by several decibels. The chart may be used for predicting audibility in certain other situations provided that minor adjustments are made to signal levels before plotting, as discussed below.

1. Alternate Probabilities of Hits and False Alarms

A detector performing as described in the chart would exhibit a probability of 0.50 of correctly detecting a signal when it occurred, and a probability of only 0.01 of incorrectly "detecting" a signal when it did not in fact occur. In some circumstances, other levels of detection performance, either more or less sensitive than this, may also be of interest. For example, one might be interested in predicting how an extremely sensitive detector (one limited only by basic physical distributions of signal and noise energy) might perform. One might also be interested in predicting how a relatively insensitive observer (one who makes poor use of available physical information) might perform.

Charts for other combinations of hit and false alarm rates would look virtually identical to Figure 6, except for a vertical shift in the curved background grid lines with respect to the rectangular signal grid. To use the present chart for other levels of detection performance, one need only add a constant to all one-third octave band signal levels before plotting. Table II

TABLE II. NUMBER OF DECIBELS TO ADD TO SIGNAL LEVEL FOR VARYING LEVELS OF DETECTION PERFORMANCE

Correct Detection Rate	False Alarm Rate 1%	5%	10%	20%
10%	3.5	8.1	-	-
20%	2.0	4.6	7.2	-
30%	1.1	3.2	4.8	8.6
40%	0.5	2.3	3.6	6.0
50%	0.0	1.5	2.6	4.4
60%	-0.5	0.9	1.8	3.2
70%	-0.9	0.3	1.1	2.3
80%	-1.3	-0.3	0.4	1.4
90%	-1.9	-1.0	-0.4	0.4
95%	-2.3	-1.5	-1.0	-0.3
99%	-3.0	-2.3	-1.9	-1.3

TABLE III. NUMBER OF DECIBELS TO ADD TO SIGNAL LEVEL FOR MULTIPLE FREQUENCY BANDS OF EQUAL DETECTABILITY

Number of Additional bands within 3dB	Adjustment
4	0.4
5	0.7
6	1.0
7	1.3
8	1.5
9	1.7
10	1.9
12	2.2
14	2.5
16	2.8
18	3.0
20	3.2
24	3.6
28	3.9

indicates how many decibels must be added to the signal level before plotting to take into consideration a variety of levels of detection performance.

2. Multiple Frequency Bands of Equal Detectability

In most cases, one or two frequency bands will have the greatest signal-to-noise ratios, and hence contribute most strongly to detectability. If, however, the plotted signal-to-noise ratios of four or more bands are all within a 3 dB range, then a human observer's detection performance can exceed that predicted by the chart. To determine this improvement, first find the frequency band where the plotted signal level is highest with respect to the plotted background. Determine from the chart the distance between the two curves in this band, in decibels. This distance will be positive if the signal is above the plotted masking noise level, but negative if the signal level curve is below the plotted masking noise level. Count the number of additional frequency bands in which this distance is algebraically within 3 dB of the highest band found. Enter Table III and read the adjustment value corresponding to the number of additional bands counted. Then add this adjustment to the signal level in the band with the highest plotted signal-to-noise ratio.

3. Tones and Narrowband Signals

If a signal spectrum contains concentrations of energy in very narrow frequency bands, it is sometimes possible for human observers to achieve a ratio of hits to false alarms for a given signal-to-noise ratio that is higher than that indicated by the chart. As a rule of thumb, adjustments to the signal

levels may be justified 1) if the energy within a one-third octave band exceeds the average energy in the two adjacent one-third octave bands by more than 3 dB; and 2) if there is good reason to believe that signal does indeed contain a tone at this frequency.

Some noise sources that exhibit such characteristics include purely tonal sources (e.g., electrical power transformers, sirens, horns, whistles, etc.); and complex sources that may radiate narrowband or quasi-tonal energy (e.g., low speed fans, rotors, or propellers) in addition to broadband energy.

In those cases in which a tonal/narrowband adjustment can be justified, the values in Table IV should be added to the actual signal spectrum before plotting on the chart.

4. Unusually short or long duration signals

The chart is intended for use in predicting the detectability of signals of durations between approximately one and ten seconds. The detectability of signals of appreciably shorter duration may be overestimated by as much as 5 dB (in the case of a signal of 100 ms duration). The chart is not intended for use in predicting the detectability of impulsive signals; neither single impulses (short duration signals with crest factors in excess of 18 dB), such as sonic booms or muzzle reports of large bore weapons; nor repetitive impulsive wavetrains, such as automatic weapons fire and helicopter blade slap.

The chart may slightly underestimate the detectability of signals of durations greater than ten seconds.

TABLE IV. NUMBER OF DECIBELS TO ADD TO SIGNAL LEVEL FOR BANDS WITH STRONG TONAL SIGNALS

Center Frequency (Hz)	Level of Tone (dB) <50	60	70	80	90
31	-2.9	-3.8	-4.9	-4.9	-4.9
40	-2.2	-3.0	-4.5	-4.9	-4.9
50	-1.5	-2.1	-3.6	-4.9	-4.9
63	-0.7	-1.2	-2.7	-4.9	-4.9
80	0.0	-0.3	-2.6	-4.1	-4.9
100	0.3	-0.3	-1.7	-3.1	-4.6
125	0.6	0.3	-0.8	-2.3	-3.8
160	0.8	0.5	0.0	-1.4	-2.9
200	1.0	0.8	0.3	-0.7	-2.2
250	1.1	1.0	0.6	0.0	-1.4
315	1.3	1.2	0.8	0.3	-0.9
400	1.4	1.2	0.8	0.2	-1.1
500	1.5	1.4	1.0	0.4	-0.6
630	1.6	1.5	1.1	0.5	-0.5
800	1.7	1.6	1.1	0.5	-0.4
1000	1.9	1.6	1.1	0.6	-0.4
1250	2.1	1.6	1.1	0.5	-0.5
1600	2.1	1.8	1.1	0.3	-0.9
2000	2.3	1.7	0.9	0.2	-1.1
2500	2.2	1.6	0.9	0.1	-1.3
3150	2.1	1.5	0.7	0.0	-1.5
4000	2.0	1.4	0.8	0.1	-1.4
5000	1.9	1.2	0.5	-0.5	-2.0
6300	1.8	1.1	0.4	-0.8	-3.0
8000	1.7	1.0	0.2	-1.0	-3.3
10000	1.7	0.9	0.2	-1.2	-3.4

C. Example of Use

Figures 7 and 8 show examples of how the chart is used. The signal and noise levels tabulated in Table V have been plotted on the rectangular and curvilinear grids, respectively. In Figure 7 the plotted signal curve exceeds that of the background. Thus the chart predicts that the signal would be detectable at least 50 percent of the time with a 1 percent false alarm rate.

Figure 8 shows a second example in which the plotted signal spectrum does not exceed the background, indicating that the signal is not detectable 50 percent of the time with a 1 percent false alarm rate. However, in this example the signal may still be detectable if the presence of pure tones and multiple frequency bands of near equal detectability is also considered. First note that the 2000 Hz band is considerably higher in level than the two adjacent bands. This observation, combined with knowledge of the signal source's ability to produce a discrete tone at that frequency, is sufficient evidence to apply a pure tone adjustment to this band. Entering Table IV with a signal level of approximately 50 dB at 2000 Hz, the adjustment of 2.3 dB is found and added to the plotted signal (as shown by the broken line).

Next, consider multiple bands. Observe that the signal and background curves are nearly parallel over a number of frequency bands. This implies that the signal is nearly equally detectable in each of these bands. A multiple band adjustment from Table III is therefore justified. Following the procedure outlined in the previous subsection, the signal in the 2000 Hz band is found to be the highest one (-1.0 dB) with respect to

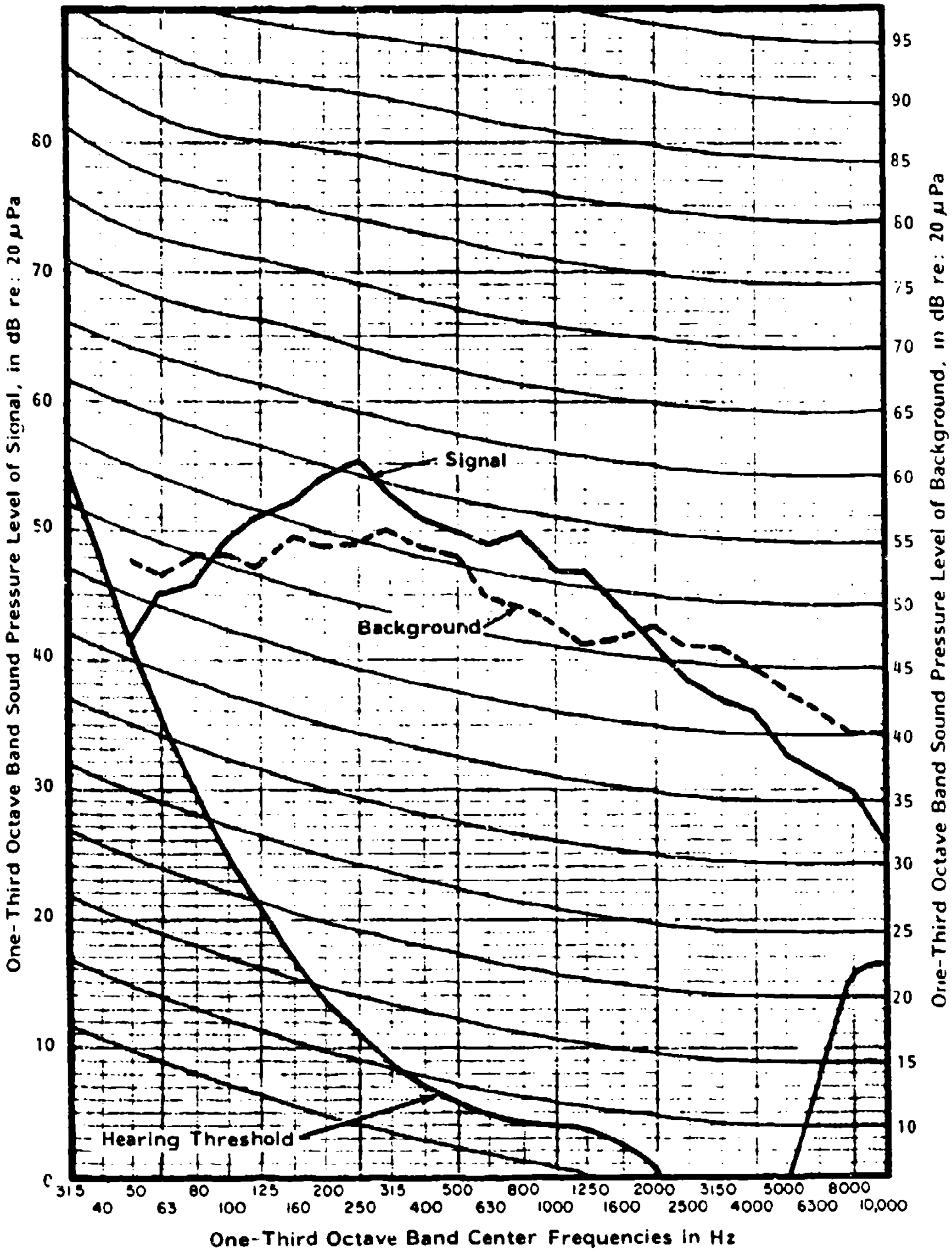

FIGURE 7. SAMPLE USE OF DETECTION CHART -- EXAMPLE A

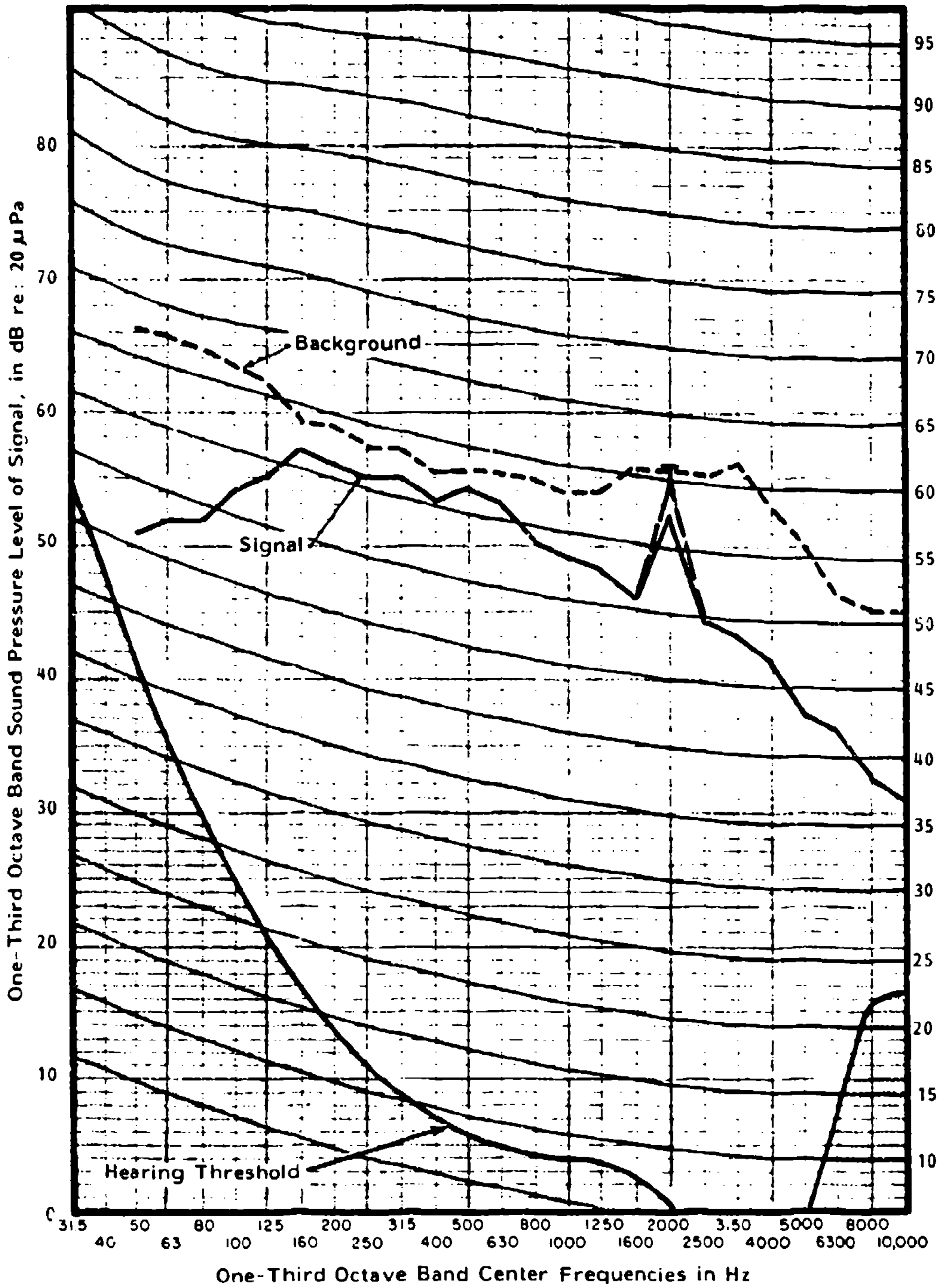

FIGURE 8. SAMPLE USE OF DETECTION CHART -- EXAMPLE B

TABLE V. SOUND PRESSURE LEVEL SPECTRA FOR TWO EXAMPLES OF USE OF DETECTION CHART

Center Frequency (Hz)	Example A		Example B	
	Signal	Background	Signal	Background
50	41 dB	43 dB	51 dB	62 dB
63	45	43	52	63
80	46	45	52	63
100	49	46	54	62
125	51	46	55	61
160	52	49	57	59
200	54	49	56	59
250	55	50	55	59
315	53	52	55	59
400	51	51	53	58
500	50	51	54	59
630	49	48	53	59
800	50	48	50	59
1000	46	46	49	58
1250	46	46	48	59
1600	44	47	46	61
2000	41	48	52	61
2500	38	46	44	61
3150	37	47	43	62
4000	36	46	41	59
5000	33	44	37	56
6300	31	43	36	52
8000	30	41	32	51
10000	26	41	31	51

the plotted background. Seven additional bands (160, 200, 250, 315, 400, 500, and 630 Hz) have signal levels which are between -1.0 dB and -4.0 dB with respect to the plotted background. Entering Table III, an adjustment of 1.3 dB is read. This value is added to the signal level in the 2000 Hz band, creating a single band which is equally detectable as a combination of the several individual bands. With the adjustment to the 2000 Hz band, the plotted signal level now exceeds that of the background. The chart thus predicts that detection would occur at least 50% of the time with a 1% false alarm rate.

REFERENCES

Abrahamson, A., "Correlation of Actual and Analytical Helicopter Aural Detection Criteria", Vol. 1, Wyle Laboratories; USAAMRDL Technical Report 74-102A, Eustis Directorate, U. S. Army Air Mobility Research and Development Laboratory, Fort Eustis, Virginia, AD B002067 (January 1975).

Fidell, S., Horonjeff, R., and Green, D., "Low Frequency Bandwidth", J. Acoust. Soc. Am., in press.

Fidell, S., Horonjeff, R., Teffeteller, S., and Green, D., "Revision of Acoustic Detection Range Prediction Model Based on Psychoacoustic Study of Low Frequency Masking", R&D Center Laboratory Technical Report No. 12543, U. S. Army Tank-Automotive Command (December 1980).

Fidell, S., Pearsons, K., and Bennett, R., "Predicting Aural Detectability of Aircraft in Noise Backgrounds", Technical Report AFFDL-TR-72-17, Air Force Flight Dynamics Laboratory, Wright-Patterson Air Force Base, Ohio (July 1972).

Fletcher, H., "Auditory Patterns", Review of Modern Physics, 12, 47-65, (1940).

Garner, W., "Auditory Thresholds of Short Tones as a Function of Repetition Rates", J. Acoust. Soc. Am. Vol. 19, pp. 600-608 (July 1947).

Green, D., McKey, M., and Licklider, J., "Detection of a Pulsed Sinusoid in Noise as a Function of Frequency", J. Acoust. Soc. Am. 31, 1446-1452 (1959).

Green, D. and Swets, D., "Signal Detection Theory and Psychophysics", John Wiley and Sons, Inc. (1966).

Hawkins, J. and Stevens, S., "The Masking of Pure Tones and of Speech by White Noise", J. Acoust. Soc. Am. 22, 6-13 (1950).

Licklider, J., "Basic Correlates of the Auditory Stimulus", HANDBOOK OF EXPERIMENTAL PSYCHOLOGY, John Wiley and Sons, Inc., pp. 985-1039 (1951).

Loewy, R., "Aural Detection of Helicopters in Tactical Situations", J. Am. Helicopter Soc. 8 (4) (1963).

Ollerhead, J., Appendix 2 of "Helicopter Aural Detectability", Wyle Laboratories, Hampton, Virginia (Prepared Under Contract DAAJ02-69-C-0083 for Eustis Directorate, U. S. Army Air Mobility Research and Development Laboratory, Fort Eustis, Virginia).

Patterson, R., "Auditory Filter Shapes Derived with Noise Stimuli, J. Acoust. Soc. Am. 59, 640-654 (March 1976).

Smith, D. and Paxson, R., "Measurements of the Radiated Noise from Sailplanes", Air Force Flight Dynamics Laboratory TM-70-3-FDDA (1970).

Swets, J., Tanner, W., and Birdsall, T., "Decision Processes in Perception", SIGNAL DETECTION AND RECOGNITION BY HUMAN OBSERVERS, John Wiley and Sons Inc., (1955).

Weber, D., "Growth of Masking and the Auditory Filter", J. Acoust. Soc. Am. 53, Vol. 62, No. 2 (August 1977).

Wegel, R. and Lane, C., "The Auditory Masking of One Pure Tone by Another and its Probable Relation to the Dynamics of the Inner Ear", Physical Review, 23(2), 266-285 (1924).